

# Reflection-type two-wavelength quantum well modulators

C.-M. TSAI, C.-P. LEE

*Department of Electronics Engineering and Institute of Electronics,  
National Chiao Tung University, Hsin-Chu 300, Taiwan, Republic of China*

*Received 24 January; revised 23 April; accepted 24 April 1997*

---

A systematic way has been developed for cavity design of reflection-type two-wavelength modulators based on coupled cavity structures. By inserting a properly designed additional reflector between the two quantum well absorbing layers with different designed operating wavelengths, two modulator structures can be combined with different operating wavelengths in one device and they can be made to operate almost independently. In this paper, three types of two-wavelength cavity designs including the simple cavity, the balanced cavity, and the decoupled cavity, are described. Their merits and drawbacks in overall modulation performance are compared. The three designs have also been realized experimentally. All of the three devices show clearly independent two-wavelength operation and the measured characteristics agree with the theoretical predictions.

---

## 1. Introduction

Surface-normal quantum well modulators based on quantum confined Stark effect (QCSE) [1] have the potential of being one of the key components for many system applications, such as optical communications [2] and interconnections [3], optical switching networks [4], and optical data processing using smart pixels [5]. Because of their compatibility with other semiconductor optoelectronic devices, quantum well modulators can easily be integrated with other devices or combined to form two-dimensional arrays. In the past, most of the modulators were built to operate at one wavelength (or one channel). For future systems, multiple channel operation and modulators which are capable of handling two wavelengths or more will be desirable. Recently we have demonstrated, for the first time, two-wavelength modulators [6, 7]. Because of the two-wavelength operation, the devices and the optical cavities have to be properly designed to accommodate the two wavelengths. In this paper, the design strategy for developing useful two-wavelength modulators is described. Three different designs are discussed and compared. The experimental results are also presented.

## 2. Basic two-wavelength operation

To achieve a two-wavelength modulator, two types of quantum wells with different operating wavelengths must be used simultaneously in one structure. But if these two modulators are put inside one simple conventional cavity, the quantum wells designed for

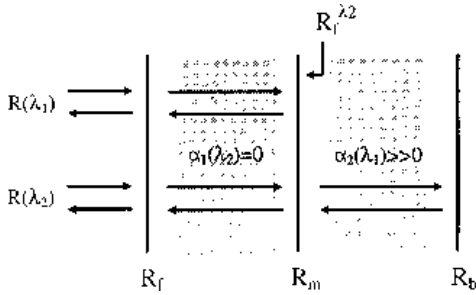


Figure 1 Schematic of proposed two-wavelength cavity.

the long wavelength will absorb the short-wavelength photons, and the resonant condition cannot be tailored for both wavelengths. Therefore, it is almost impossible to achieve reasonable modulation performance by using such a simple cavity.

Our proposed two-wavelength modulator is schematically shown in Fig. 1. An additional middle reflector is added in the device to separate the two absorbing regions. The quantum wells for the short wavelength  $\lambda_1$  is put in the front cavity and the quantum wells for the long wavelength  $\lambda_2$  is put in between the middle reflector and the back mirror. The figure also gives the basic description of our proposed two-wavelength operation. As shown in this figure, if the reflectivity of the middle mirror is high at  $\lambda_1$ , due to the large absorption coefficient of the quantum wells in the rear cavity, the modulation characteristics for  $\lambda_1$  are determined mostly by the front cavity. On the other hand, for operation at long wavelength  $\lambda_2$ , the whole device structure acts like a coupled cavity because the quantum wells in the front cavity are transparent at this wavelength.

From the explanation given above, one can see that the whole structure needs to be designed in such a way so that the front cavity satisfies the resonant condition for  $\lambda_1$  and both the front cavity and the rear cavity satisfy the resonant condition for  $\lambda_2$ . A complicated matching condition has to be satisfied in order to obtain a proper operation. But, as will be described later, if we use a properly designed middle reflector, we can obtain a simpler matching condition for device fabrication.

### 2.1. Simple cavity design

For convenience, we first consider a simple two-wavelength modulator design, in which the reflectivities of the front mirror and the middle reflector are the same for both wavelengths. The reflectivities of the mirrors as functions of wavelength are schematically shown in Fig. 2a. The mirrors needed are broad band, which can be easily achieved by Bragg reflectors.

Before entering into more detailed analysis, let us first take an overview of the well-established design rule for a conventional asymmetric Fabry–Pérot modulator (AFPM). The operation of the AFPM makes use of the QCSE in the MQWs, which is placed in between the front and the back mirrors, to control the reflectivity of a Fabry–Pérot cavity at one of its resonances. A modulation of the absorption coefficient of the QWs yields a modulation of the overall reflectivity  $R$  according to [8]:

$$R = \frac{R_f(1 - R_x/R_f)^2}{(1 - R_x)^2}$$

$$R_x = \sqrt{R_f R_b} e^{-\alpha d}$$

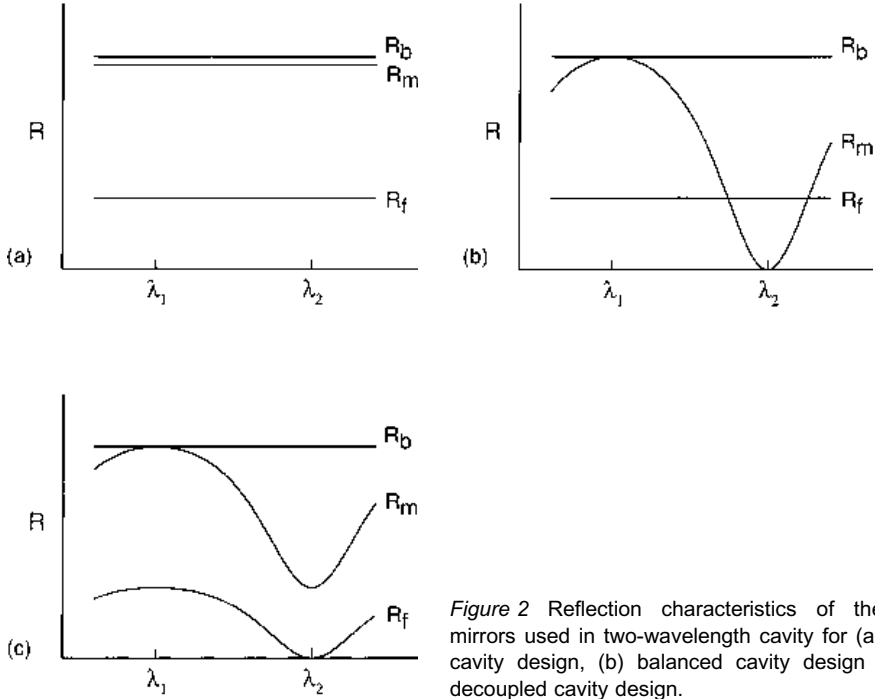


Figure 2 Reflection characteristics of the three mirrors used in two-wavelength cavity for (a) simple cavity design, (b) balanced cavity design and (c) decoupled cavity design.

where  $R_f$  is the front- and  $R_b$  the back-mirror reflectivity,  $\alpha$  is the absorption coefficient and  $d$  the thickness of the absorbing layer respectively. For AFP cavity with zero absorber incorporated, the overall reflectivities for various  $R_f$  and  $R_b$  values are plotted in Fig. 3a. When the front ( $R_f$ ) and the effective-back mirror ( $R_b^{eff} = R_b e^{-2\alpha d}$ ) reflectivities are equal at a resonant wavelength, the reflection from the AFP cavity becomes zero. From this

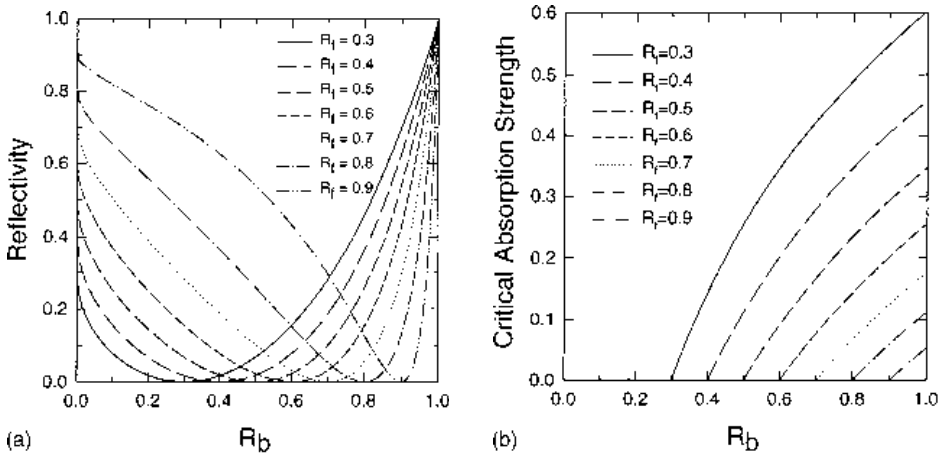


Figure 3 Calculated (a) overall reflectivity ( $\alpha d = 0$ ) and (b) critical absorption strength ( $R_f \leq R_b$ ) for an AFP cavity with various front-mirror ( $R_f$ ) and back-mirror ( $R_b$ ) reflectivities.

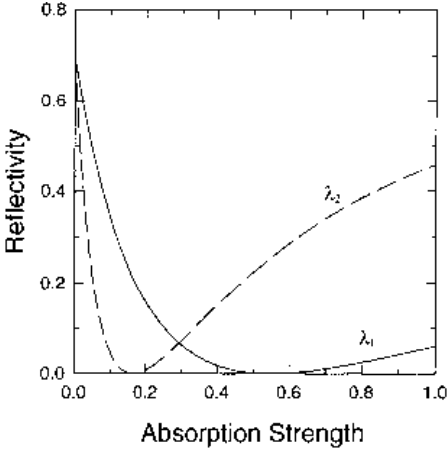


Figure 4 Calculated reflectivities as functions of absorption strength at  $\lambda_1$  and  $\lambda_2$  for simple cavity design with  $R_f = 0.3$ ,  $R_m = 0.9$  and  $R_b = 0.968$ .

relation, for the AFPM with  $R_f < R_b$ , we obtained the critical absorption strength  $[\alpha d]_c$  required for zero-reflection as given by

$$[\alpha d]_c = \ln \sqrt{\frac{R_b}{R_f}}$$

The calculated results as functions of the reflectivities of the front mirror and the back mirror are also shown in Fig. 3b.

In our two-wavelength structure, the front cavity is designed to satisfy the resonant condition at both  $\lambda_1$  and  $\lambda_2$ . For the long-wavelength operation, the effective front-mirror reflectivity  $R_f^{22}$  seen by the  $\lambda_2$  absorbing region (the rear cavity) is equal to the overall reflectivity of the front cavity, or the ideal on-state reflectivity for the short wavelength,  $\lambda_1$ . For example, from Fig. 3a, one can see that a front cavity with  $R_f = 0.3$  and  $R_m = 0.9$  gives an  $R_f^{22}$  of 0.7 for the rear cavity. If we want both wavelengths to have a similar ideal on-state reflectivity, 0.7 in this case, the bottom mirror needs to have a reflectivity of 0.968. From Fig. 3b, it is clear that for a cavity with higher  $R_f$  and  $R_b$  values a relatively smaller absorption strength is enough to turn the device off. We have simulated the modulation characteristics (reflectivity as a function of the absorption strength) for the two wavelengths. Figure 4 shows the result. The critical absorption strength is 0.55 for the  $\lambda_1$  (the short wavelength) cavity and 0.175 for the  $\lambda_2$  (the long wavelength) cavity. The large difference between the two is a direct result of the difference in cavity confinement in the two cavities. For the front  $\lambda_1$  cavity, it is confined by a high-reflection back mirror and  $R_f = 0.3$  front mirror. This forms a relatively low-finesse resonant cavity compared with the rear long-wavelength cavity which has a front-mirror reflectivity  $R_f^{22}$  of 0.7. From the above analysis, we know that such a kind of cavity design will result in a large difference in the operating voltage for the two wavelengths because of the difference in the critical absorption strength.

## 2.2. Balanced cavity design

In real applications, it is desirable to have similar modulation characteristics for the two wavelengths. In the simple cavity design described above, the front-mirror reflectivities for

the two wavelengths are different resulting in different modulation characteristics. To solve this problem, one has to choose a design which gives the same front-mirror reflectivities for the two wavelengths.

If we have a middle mirror which is highly reflective for  $\lambda_1$  but transparent for  $\lambda_2$ , the long-wavelength light will not feel the existence of the middle mirror but instead sees the front mirror of the front cavity directly. So in this case, both cavities have a same front-mirror reflectivity. If the reflectivity of the middle mirror for  $\lambda_1$  is the same as the bottom-mirror reflectivity for  $\lambda_2$ , the two cavities will have the same cavity confinements and we have a balanced design for the two wavelengths. Both cavities will exhibit similar modulation performance in on-off characteristics and a similar operating voltage can be expected for both wavelengths. The reflectivities of the three mirrors as functions of wavelength are schematically shown in Fig. 2b. With this kind of cavity design, the matching condition for  $\lambda_2$  becomes simpler. Only the whole structure, but not the front cavity and the rear cavity separately, needs to satisfy the resonant condition for  $\lambda_2$ . This greatly simplifies the growth procedure. However, to realize such a balanced design, we need a filter-like reflector which is wavelength dependent.

The reflection characteristics needed for the middle reflector in a balanced design can be realized with a resonant cavity structure. We can put two identical Bragg reflectors face to face with a small  $\lambda_2/2$ -thick cavity in between. In this case the reflector (actually a cavity) will have zero reflectance at  $\lambda_2$  with a high reflectivity at  $\lambda_1$ . The design of such a reflector will be described in detail in Section 3.

### 2.3. Decoupled cavity design

In the balanced cavity design, the cavities of the two wavelengths share the same front mirror. The two cavities are still coupled together and one cannot independently design each cavity. To eliminate this coupling effect, we introduce the third design for the two-wavelength modulator. The reflectivities of the three mirrors used in this design have the wavelength-dependent characteristics shown in Fig. 2c. The front mirror's reflectivity is also designed to be wavelength dependent. This mirror serves as a front reflector for the first cavity ( $\lambda_1$ ) but is transparent for  $\lambda_2$ . The middle mirror, which serves as the back reflector for the first cavity, is the front reflector for the second cavity ( $\lambda_2$ ). In this way, the two cavities are totally decoupled and physically separated. We can independently design the cavity length and the mirror reflectivity for each wavelength.

## 3. Reflector design scheme

To realize a reflector with desired reflectivities as the two designed wavelengths, we need to have a systematic design methodology. In general, our middle reflector needs to have a high reflectivity at  $\lambda_1$  and some other value at  $\lambda_2$ . This is quite different from the conventional single-wavelength design, where we only need to have a broadband reflector with a specific reflectivity within certain wavelength range. Now we have to be concerned with two wavelengths, where the reflector performs differently. To achieve such filter-type reflector characteristics, we use two Bragg reflectors stacked face to face, similar to an AFP cavity design. We can build the cavity in such a way that it resonates at  $\lambda_2$  so the reflectivity is at a minimum, and is away from resonance at  $\lambda_1$  so the reflectivity is high. In this way, the reflectivities for the two wavelengths will be very different. Let us consider such an FP reflector consisting of two Bragg mirrors, each with reflectivity of  $R_1$  and  $R_2$  respectively, and an interlayer with refractive index  $n$  and

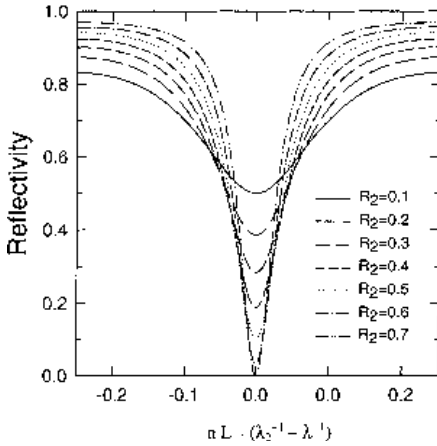


Figure 5 Calculated reflection characteristics for an AFP cavity composed of two mirrors with reflectivities of  $R_1 = 0.7$  and various  $R_2$  values. The refractive index,  $n$ , was treated as a constant in our calculation.

thickness  $L$  in between. And suppose we build this cavity for resonance at  $\lambda_2$ . If we keep  $R_1$  at 0.7, which makes sure that the overall reflectivity for  $\lambda_1$  is high enough for a proper on-state performance, the reflection characteristics with various  $R_2$  values are shown in Fig. 5. As shown in the figure, while keeping a high reflectivity at  $\lambda_1$ , we can adjust the reflectivity at  $\lambda_2$  to any desired value (the minimum point) by using such an AFP cavity structure.

#### 4. Experimental results

All the three structures described above for two-wavelength modulation have been realized experimentally. The layers were grown by MBE. In some of the structures, the reflectivities of the mirrors (and cavities) were monitored *in situ* to ensure the growth of the structures with the right characteristics.

##### 4.1. Modulator with simple cavity design

The whole structure is schematically shown in Fig. 6a. The growth started with 15 periods of  $\text{Al}_{0.1}\text{Ga}_{0.9}\text{As}(625\text{\AA})/\text{AlAs}(732\text{\AA})$  DBR mirror which was followed by the 33 periods of  $\text{In}_x\text{Ga}_{1-x}\text{As}(100\text{\AA})/\text{Al}_{0.3}\text{Ga}_{0.7}\text{As}(45\text{\AA})$  quantum wells designed for long-wavelength operation. Then an important matching procedure in layer thickness was followed for reaching resonance at our desired operating wavelength, here the wavelength of 885 nm was chosen. The middle reflector was composed of ten pairs of DBR stack and then the short-wavelength quantum-well region, 90 periods of  $\text{GaAs}(80\text{\AA})/\text{Al}_{0.3}\text{Ga}_{0.7}\text{As}(45\text{\AA})$ , were sequentially grown on the matched cavity structure. The non-biased excitonic wavelength was 840 nm. The second operating wavelength we chose was 855 nm. By adjusting the layer thickness for simultaneous operations at 885 nm and 855 nm, the total thickness was about 6  $\mu\text{m}$ . In this structure, the middle reflector was wideband and had a high reflectivity of over 80% covering a range from 850 nm to 930 nm. Our designed wavelengths were both within this high-reflection band. The air-interface reflection supported a reflectivity of  $\sim 0.3$  for both wavelengths. While this is the front-mirror reflectivity for 855 nm, the calculated front-mirror reflectivity is around 0.6 for 885 nm. Owing to the very different front-mirror reflectivities, this device was expected to exhibit strong unbalanced modulation performance.

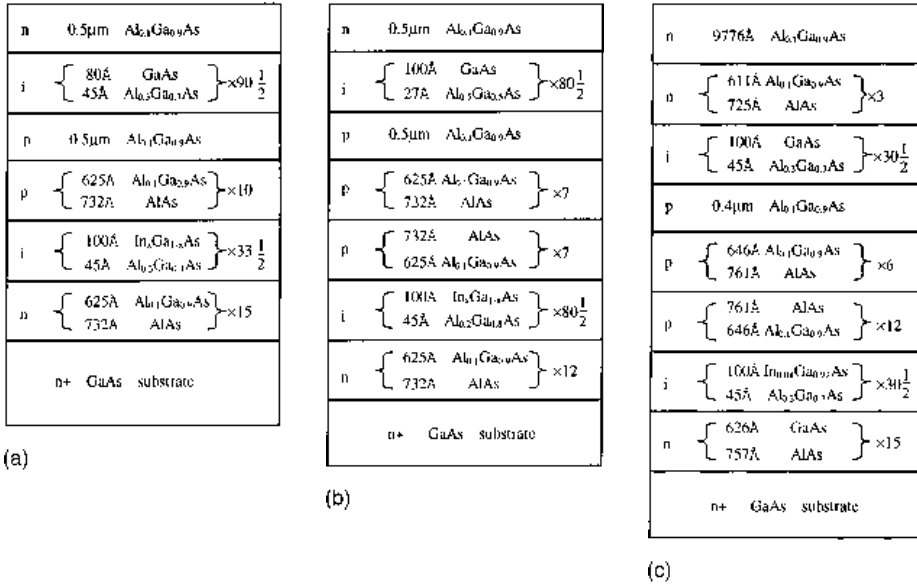


Figure 6 Grown device structures of fabricated two-wavelength modulators with (a) simple cavity, (b) balanced cavity and (c) decoupled cavity design.

After the layer growth, the device was fabricated by two mesa-etching steps to define the ohmic contact for each modulator separately. Figure 7 shows the modulated reflection spectra with each modulator biased separately. As clearly shown in the figure, the two-wavelength operation at wavelengths of 856 nm and 886 nm was achieved. Each modulator operated almost independently without any significant crosstalk. For the operation at 856 nm, an excellent reflectivity change of 70% was obtained for a bias voltage of 19 V. For the 886 nm operation, however, only 5 V was needed to cause a 54% change in

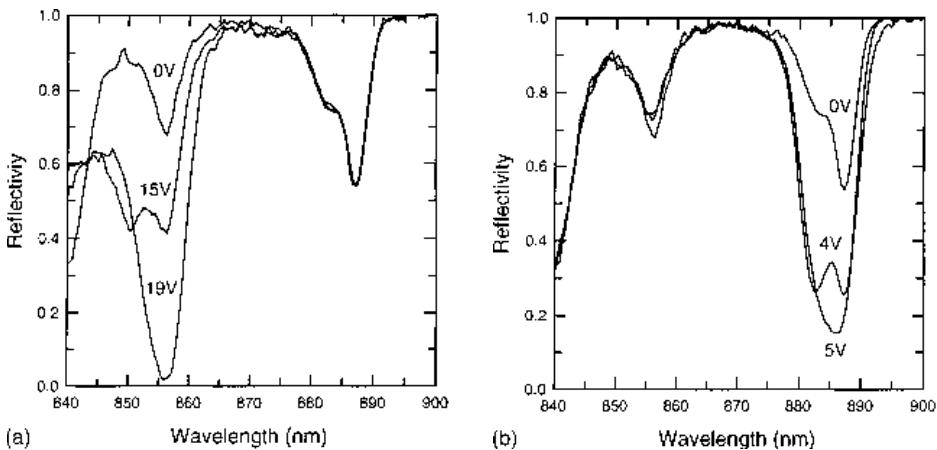


Figure 7 Reflection spectra of two-wavelength modulator with simple cavity design under various biasing voltages (a) on the upper short-wavelength QWs and (b) on the lower long-wavelength QWs.

reflectivity. The difference in operating voltage is due to the different thicknesses used in the quantum well regions and also the different mirror reflectivities in the two cavities discussed earlier.

#### 4.2. Modulator with balanced cavity design

The complete layer structure of the grown device is shown in Fig. 6b. The whole structure started with 12 pairs of n-type  $\text{Al}_{0.1}\text{Ga}_{0.9}\text{As}(625\text{\AA})/\text{AlAs}(732\text{\AA})$  DBR mirror which is followed by 80 periods of undoped  $\text{In}_x\text{Ga}_{1-x}\text{As}(100\text{\AA})/\text{Al}_{0.2}\text{Ga}_{0.8}\text{As}(45\text{\AA})$  quantum-well region for the long-wavelength operation. The filter-type middle mirror comprised two face-to-face DBR stacks, each containing seven pairs of p-type  $\text{Al}_{0.1}\text{Ga}_{0.9}\text{As}(625\text{\AA})/\text{AlAs}(732\text{\AA})$ . These two DBR stacks form a resonant cavity with the resonant wavelength at 895 nm. In other words, this middle mirror is transparent at 895 nm, the designed value for the long-wavelength operation. At the same time, this mirror was designed to support a high reflectivity of over 85% at 860 nm, the designed value for the short-wavelength operation. The second 80 periods  $\text{GaAs}(100\text{\AA})/\text{Al}_{0.5}\text{Ga}_{0.5}\text{As}(27\text{\AA})$  quantum-well layer was grown next. Finally an n-type  $\text{Al}_{0.1}\text{Ga}_{0.9}\text{As}$  contact layer was grown. The front mirror was again the semiconductor–air interface.

In the same manner, two mesa-etching steps were followed to define separately the ohmic contact for each modulator. Measured reflection spectra were shown in Fig. 8. Two-wavelength operation was also clearly observed in such a device without any significant crosstalk. As we can see from the figure, owing to this balanced cavity design, the bias voltages needed to turn off the device for both wavelengths are similar. Reflectivity changes of over 50% were also achieved at both of the operating wavelengths.

#### 4.3. Modulator with decoupled cavity design

The structure of the device is shown in Fig. 6c. The two quantum-well regions were 30 pairs of  $\text{GaAs}(100\text{\AA})/\text{Al}_{0.3}\text{Ga}_{0.7}\text{As}(45\text{\AA})$  and  $\text{In}_{0.08}\text{Ga}_{0.92}\text{As}(100\text{\AA})/\text{Al}_{0.3}\text{Ga}_{0.7}\text{As}(45\text{\AA})$  for the short wavelength and the long wavelength, respectively. In this decoupled struc-

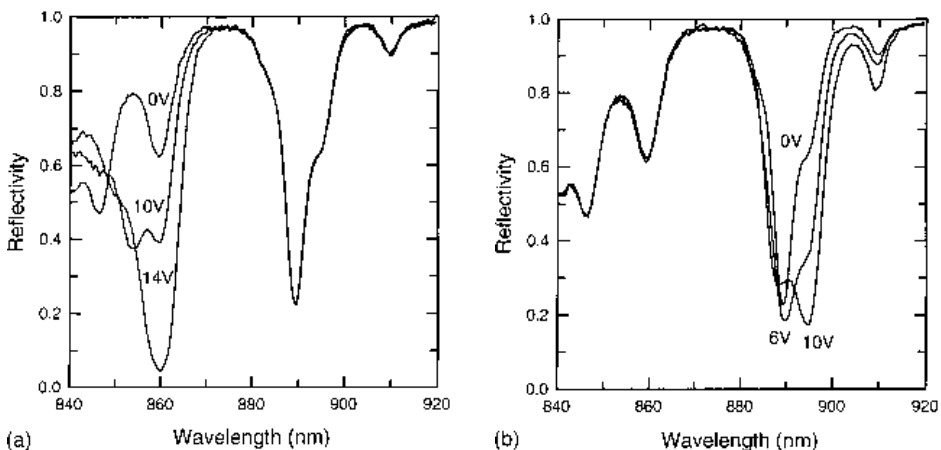


Figure 8 Reflection spectra of two-wavelength modulator with balanced cavity design under various biasing voltages (a) on the upper short-wavelength QWs and (b) on the lower long-wavelength QWs.



ture, the reflectivities of both the front mirror and the middle mirror have to be wavelength dependent. For the front mirror, we used a structure consisting of three pairs of  $\text{Al}_{0.1}\text{Ga}_{0.9}\text{As}(611\text{\AA})/\text{AlAs}(725\text{\AA})$  quarter wavelength ( $\lambda_1/4$ ) stacks plus an  $\text{Al}_{0.1}\text{Ga}_{0.9}\text{As}$  layer with a thickness of  $4\lambda_1$ . The calculated reflectivity at  $\lambda_2$ , 905 nm (the long wavelength), was close to zero while the reflectivity at  $\lambda_1$  (865 nm for the short wavelength) was close to 0.6. The middle mirror is an AFP structure, in which one of the reflectors is six pairs of  $\text{Al}_{0.1}\text{Ga}_{0.9}\text{As}/\text{AlAs}$  DBR stack and the other is 12 pairs of  $\text{Al}_{0.1}\text{Ga}_{0.9}\text{As}(646\text{\AA})/\text{AlAs}(761\text{\AA})$  DBR stack. The two DBRs were put face-to-face to create a resonant cavity. The resonant wavelength was at the designed long wavelength, 905 nm, and the reflectivity at this wavelength was 0.57. The estimated reflectivity at 865 nm was 0.94. The bottom mirror was 15 pairs of  $\text{GaAs}(626\text{\AA})/\text{AlAs}(757\text{\AA})$  DBR stack with a calculated reflectivity of over 0.95.

In the decoupled structure described above, the cavity for the short wavelength and the cavity for the long wavelength had similar mirror reflectivities and similar cavity lengths. The modulation characteristics for both wavelengths are shown in Fig. 9. The voltages needed to turn off the device at the two wavelengths are very similar (at around 4.5 V). The reason that the voltage needed here is lower than those used in the previous two structures is the relatively higher front-mirror reflectivity used in the present structure. In this structure both wavelengths see a front-mirror reflectivity of  $\sim 0.6$ , while the other two structures rely on the air–semiconductor interface as the front mirror which has a reflectivity of  $\sim 0.3$ .

## 5. Conclusions

Three design approaches for realization of two-wavelength modulators have been described. Detailed design procedures and related cavity properties have been given for each of the three types of designs, including the simple cavity design, the balanced cavity design, and the decoupled cavity design. Two-wavelength normally-on modulators based on these three designs were experimentally demonstrated. Clear two-wavelength modulation characteristics have been achieved. The operation of the devices and the results agree with

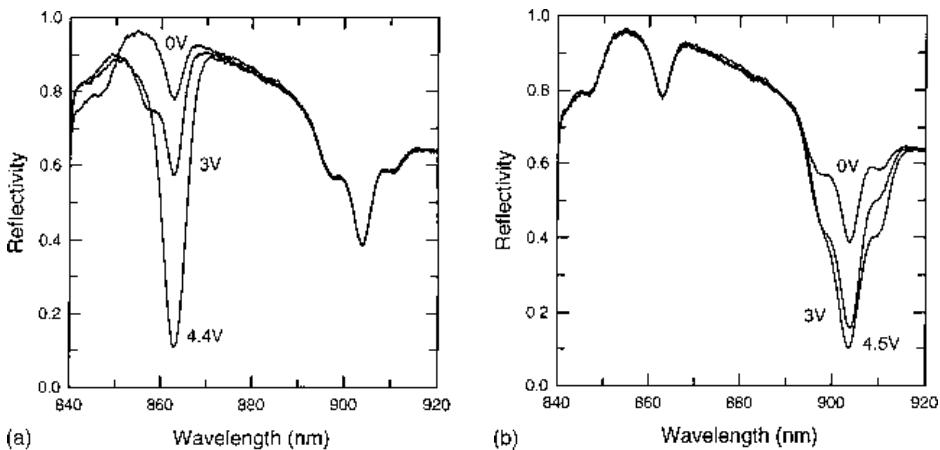


Figure 9 Reflection spectra of two-wavelength modulator with decoupled cavity design under various biasing voltages (a) on the upper short-wavelength QWs and (b) on the lower long-wavelength QWs.

the theoretical design considerations. Although the wavelengths used in the demonstration are around 855–905 nm, the principle is equally applicable to longer wavelengths, which are more useful for long-distance communication applications. The wavelength spacing in the demonstrated devices is around 300 nm; closer spacing should be possible through improved design in the quantum wells and the resonant cavities. The large wavelength spacing, although it may impede its applications for dense WDM systems, is still acceptable for many applications such as optical image processing, and optical interconnections. The two-wavelength modulators demonstrated in this paper will open up many possible applications which require parallel and large data throughput.

### Acknowledgement

This work is supported by the National Science Council of the Republic of China under contract NSC86-2215-E009-010.

### References

1. D. A. B. MILLER, D. S. CHEMLA, T. S. DAMEN, A. S. GOSSARD, W. WIEGMANN, T. H. WOOD and C. A. BURRUS, *Phys. Rev. B* **32** (1985) 1043.
2. C. C. BARRON, C. J. MAHON, B. J. THIBEAULT, G. WANG, W. JIANG, LARRY A. COLDREN and J. E. BOWERS, *IEEE J. Quantum Electron.* **QE-31** (1995) 1484.
3. A. J. MOSELEY, M. Q. KEARLEY, R. C. MORRIS, D. J. ROBBINS, J. THOMPSON and M. J. GOODWIN, *Electron. Lett.* **28** (1992) 12.
4. J. E. MIDWINTER, *IEE Proc.* **134** (1987) 261.
5. A. L. LENTINE and D. A. B. MILLER, *IEEE J. Quantum Electron.* **QE-29** (1993) 655.
6. C. M. TSAI and C. P. LEE, *Electron. Lett.* **33** (1997) 611.
7. C. M. TSAI and C. P. LEE, accepted for publication *IEEE Photon. Technol. Lett.* (July 1997).
8. M. WHITEHEAD, G. PARRY and P. WHEATLEY, *IEEE Proc. J.* **136** (1989) 52.